Scalar decay in two-dimensional chaotic advection and Batchelor-regime turbulence

D. R. Fereday and P. H. Haynes
Department of Applied Mathematics and Theoretical Physics, University of Cambridge, Wilberforce Road, Cambridge CB3 OWA, United Kingdom

(Received 9 January 2004; accepted 23 August 2004; published online 21 October 2004)

This paper considers the decay in time of an advected passive scalar in a large-scale flow. The relation between the decay predicted by "Lagrangian stretching theories," which consider evolution of the scalar field within a small fluid element and then average over many such elements, and that observed at large times in numerical simulations, associated with emergence of a "strange eigenmode" is discussed. Qualitative arguments are supported by results from numerical simulations of scalar evolution in two-dimensional spatially periodic, time aperiodic flows, which highlight the differences between the actual behavior and that predicted by the Lagrangian stretching theories. In some cases the decay rate of the scalar variance is different from the theoretical prediction and determined globally and in other cases it apparently matches the theoretical prediction. An updated theory for the wavenumber spectrum of the scalar field and a theory for the probability distribution of the scalar concentration are presented. The wavenumber spectrum and the probability density function both depend on the decay rate of the variance, but can otherwise be calculated from the statistics of the Lagrangian stretching history. In cases where the variance decay rate is not determined by the Lagrangian stretching theory, the wavenumber spectrum for scales that are much smaller than the length scale of the flow but much larger than the diffusive scale is argued to vary as $k^{-1+\rho}$, where k is wavenumber, and ρ is a positive number which depends on the decay rate of the variance γ_2 and on the Lagrangian stretching statistics. The probability density function for the scalar concentration is argued to have algebraic tails, with exponent roughly -3 and with a cutoff that is determined by diffusivity κ and scales roughly as $\kappa^{-1/2}$ and these predictions are shown to be in good agreement with numerical simulations. © *2004 American Institute of Physics*.
[DOI: 10.1063/1.1807431]

I. INTRODUCTION

Several recent papers[1–4] have used theories based on the statistical distribution of stretching histories following fluid particles to predict the evolution of passive scalars (undergoing advection and diffusion) in large-scale flows in the large-Peclet-number limit (i.e., weak diffusion). These theories predict the evolution of a range of measures of the scalar field, including probability distributions for both the scalar concentration and its gradient, structure functions and spatial power spectra, in both the case of a freely evolving initial value problem and the case of a forced problem where the scalar field reaches a statistical equilibrium. We refer to these theories as "Lagrangian stretching theories."

By "large-scale flow" we mean that the velocity field has a well-defined smallest spatial scale that is much larger than the smallest scale attained by the scalar field (the latter scale being determined jointly by advective stretching and diffusion). One example is the "Batchelor regime" of three-dimensional turbulence, in which the Schmidt number (the ratio of the momentum diffusivity to the scalar diffusivity) is large, so that the minimum scale of the velocity field, the Kolmogorov scale, is larger than the minimum scale of the scalar field. Another is that commonly known as chaotic advection,[5–7] where velocity fields, e.g., time-periodic fields, with simple spatial structure give rise to scalar fields with very small scales. Conversely, an example of a flow that is not "large-scale" is three-dimensional turbulence when the scalar diffusivity is of the same order of magnitude as the momentum diffusivity (or larger than it).

The important differences between large-scale flow and other cases are emphasized in the review by Falkovich, Gawedzki, and Vergassola[4] (who use the terminology "smooth" and "nonsmooth"). We note here that while large-scale flow is more tractable than other cases and is not directly relevant to fundamental theoretical issues in three-dimensional turbulence, it has many practical applications, e.g., in flows in the atmosphere, ocean and Earth's interior and in important classes of chemical engineering problems.

The Lagrangian stretching theories exploit the difference in scale between the velocity field and the scalar field to argue that, by transforming to a frame of reference moving with a relevant fluid element, the problem for the scalar field is equivalent, locally, to that for a scalar field in a flow that is a linear function of space. This problem may be solved for a given stretching history, i.e., a given time history of the velocity gradient tensor for the linear flow, and then the statistics of the scalar field deduced by considering all realization of the stretching history, i.e., following all possible fluid elements.

A recent paper by Fereday *et al.*[8] throws doubt on the validity of the Lagrangian stretching theories for predicting

decay rates in the initial-value problem. That paper considers a prototype one-dimensional problem in which advection is represented by a baker's map, but notes the significance of disagreements between local stretching theories and explicit calculations of scalar decay in two-dimensional flows by Pierrehumbert,[9] who demonstrated the emergence of a dominant exponentially decaying structure in the scalar field that he called a "strange eigenmode."[9,10] In mathematical terms the decay rate is determined by the eigenvalues (or more strictly the Liapunov exponents) of the advection-diffusion operator (in the limit of small diffusivity). See Childress and Gilbert[11] and Sukhatme and Pierrehumbert[12] for more details on the mathematical background. Sukhatme and Pierrehumbert[12] demonstrate inconsistencies between the numerical results and the Lagrangian stretching theories, particularly that at large times the behavior of higher moments of the scalar field predicted by the theories[2–4] are inconsistent with the probability distribution function for values of the scalar field implied by the simulations.

This paper further considers the initial-value problem for scalars in large-scale flows. It shows that the Lagrangian stretching theories cannot always predict the long-time decay rate of the strange eigenmode. It generalizes a previous theoretical prediction for the scalar wavenumber spectrum and gives a theoretical prediction for the probability density function for the scalar concentration and compares the predictions with numerical simulations.

The structure of this paper is as follows. Section II gives a general discussion of the advection-diffusion problem, with the aim of clarifying both the progress allowed by the Lagrangian stretching theories and the limitations of such theories. Section III summarizes the predictions of the Lagrangian stretching theories. Section IV describes numerical simulations of the initial-value problem for the advection-diffusion problem in two dimensions, following previous work in this field by using a flow that is aperiodic in time. Section V considers the Cramer "rate function" describing the probability distribution of stretching factors, which plays a central role in the Lagrangian stretching theories and is also important for the results presented here. Section VI exploits the previous discussion in Sec. II of the paper to present an updated theory for the wavenumber spectrum of the scalar concentration field and a theory, compared against numerical simulation, for the probability density function for the scalar concentration. Section VII discusses the results of the paper and their implications.

II. ADJOINT PROBLEM FOR INITIAL VALUE PROBLEM AND IMPLICATIONS

We consider the initial value problem for the advection-diffusion equation, i.e.,

$$\chi_t + \mathbf{u}(\mathbf{x},t) \,.\, \nabla_{\mathbf{x}}\chi - \kappa\nabla^2_{\mathbf{x}}\chi = 0 \tag{1}$$

with $\chi(\mathbf{x},t)$ the scalar concentration, $\mathbf{u}(\mathbf{x},t)$ the velocity field, assumed to be a given function of space $\mathbf{x}$ and time t and to be incompressible, and κ the diffusivity, assumed constant. Equation (1) is to be solved given the initial condition that $\chi(\mathbf{x},0)=\chi_0(\mathbf{x})$, where χ_0 is a given function of space. Without loss of generality we shall assume that the integral of $\chi_0(\mathbf{x})$ over the domain is zero.

The solution to (1) may be written as

$$\chi(\mathbf{x},t) = \int d\mathbf{y}\chi_0(\mathbf{y})\mathcal{G}(\mathbf{x},t,\mathbf{y},0) \tag{2}$$

where the Green's function $\mathcal{G}(\mathbf{x},t,\mathbf{y},s)$ is the solution to (1) with initial condition $\chi(\mathbf{x},s)=\delta(\mathbf{x}-\mathbf{y})$.

One important property of $\mathcal{G}(\mathbf{x},t,\mathbf{y},s)$ is that it is not only the solution of an advection-diffusion equation in which $\mathbf{x}$ and t are space and time variables and $\mathbf{y}$ and s are variables indicating where and when the function defining the initial conditions is to be evaluated, but it is also the solution of an adjoint advection-diffusion equation in which the roles of these two pairs of variables are reversed. Thus $\mathcal{G}(\mathbf{x},t,\mathbf{y},s)$ is also the solution to the equation

$$\chi_s + \mathbf{u}(\mathbf{y},s) \,.\, \nabla_{\mathbf{y}}\chi + \kappa\nabla^2_{\mathbf{y}}\chi = 0 \tag{3}$$

with initial condition $\chi(\mathbf{y},t)=\delta(\mathbf{y}-\mathbf{x})$. Note that the sign of the diffusive term in (3) is reversed relative to that in (1), implying that just as (1) may be integrated only forward in t, (3) may be integrated only backward in s.

It follows from (2) that the value of tracer concentration at a particular point $\mathbf{x}$ and at time t is a weighted integral over the initial field, where the weighting function is the Green's function $\mathcal{G}(\mathbf{x},t,\mathbf{y},s)$, determined by backwards integration in s of (3) from time $s=t$ to time $s=0$, with "initial" condition that $\mathcal{G}(\mathbf{x},t,\mathbf{y},t)=\delta(\mathbf{y}-\mathbf{x})$.

The relation between (1)–(3) is well known, but we reiterate it here since it provides a framework in which to analyze solutions of (1) in which the relation between and the limitations of different approximation procedures can be made absolutely clear.

Familiar physical intuition on the advection-diffusion equation, applied to (3) may be used to predict the evolution of $\mathcal{G}(\mathbf{x},t,\mathbf{y},s)$ as s decreases from t. It is useful to consider the region of $\mathbf{y}$ space where $\mathcal{G}(\mathbf{x},t,\mathbf{y},s)$ takes significant values, i.e., the region that gives a significant contribution to the integral in (2), as the "domain of influence" on $\mathbf{x}$ (at time t) and to identify ranges of $t-s$ in which the domain of influence has different characteristics.

For $t-s$ small enough (defined here as regime I), diffusion dominates and the domain of influence spreads isotropically. Then for $t-s \gtrsim S_{\mathrm{loc}}^{-1}$ (defined here as regime II), where S_{loc} is the time-averaged stretching rate following the backwards trajectory from $\mathbf{x}$, advection becomes important and domain of influence on $\mathbf{x}$ is stretched in the form of a elliptical filament, whose width remains at an equilibrium width of order $(\kappa/S_{\mathrm{loc}})^{1/2}$ determined by the balance between advection and diffusion and whose length increases exponentially with $t-s$ as $(\kappa/S_{\mathrm{loc}})^{1/2}e^{S_{\mathrm{loc}}(t-s)}$. Regimes I and II are well described by an analysis in a coordinate system where the origin follows a fluid particle trajectory backwards in time from the point $\mathbf{x}$ and the velocity field is approximated as a linear function of space. We discuss this in more detail in Sec. III.

Eventually, however, the length of the filamentary region corresponding to the domain of influence reaches the length

scale L_{flow} on which the flow varies. This occurs when $(\kappa/S_{\text{loc}})^{1/2}e^{S_{\text{loc}}(t-s)} \sim L_{\text{flow}}$, i.e., $t-s \sim \frac{1}{2}S_{\text{loc}}^{-1}\ln(S_{\text{loc}}L_{\text{flow}}^2/\kappa)$. At this stage the velocity field can no longer be approximated as a linear function of space and the filamentary region begins to curve and fold (defined as regime III). It therefore seems unlikely this regime can be fully captured by theories that follow the stretching histories of individual fluid parcels and approximate the velocity field as a linear function of space.

The details of what happens subsequently depends on the transport and mixing properties of the flow. Here we shall consider flows that are globally mixing in the sense that a small material area is deformed by the flow such that at sufficiently large times it intersects an arbitrarily chosen area in the flow domain. In other words we shall assume that there are no transport barriers (barriers to purely advective transport) that divide the flow into disjoint regions. It follows that the filamentary area corresponding to the domain of influence of any point $\mathbf{x}$ is repeatedly stretched and folded as s decreases from t until it covers the whole domain. The period during which the filamentary area visits only part of the domain will be regarded as belonging to regime III. The final regime, beyond the time at which domain of influence has expanded to cover the whole flow domain, is defined as regime IV. The structure of the domain of influence in this final regime might be described as "packed filaments" in the terminology of Sukhatme and Pierrehumbert.[12] The different regimes of behavior are depicted schematically in Fig. 1.

In regime III the domain of influence samples stretching rates associated with many parts of the flow and an estimate for the time spent in regime III, i.e., the time taken for the area of the domain of influence to increase to L_{flow}^2, is given by $\frac{1}{2}S_{\text{glob}}^{-1}\ln(L_{\text{flow}}^2 S_{\text{loc}}/\kappa)$, where S_{glob} is the stretching rate averaged over the entire flow.

Note that if there are transport barriers in the flow, then the domain of influence of a given point will eventually cover the whole flow domain, but the time scales for penetration of the barriers by the domain of influence will depend strongly on the diffusivity κ.

Now consider the implications for the evolution of the concentration, which is a weighted integral of the initial concentration field over the domain of influence. Denote the length scale of variation of the initial scalar field $\chi_0(\mathbf{x})$ by L_{χ_0}. At early times (regimes I and II) the domain of influence on $\mathbf{x}$ has a scale much smaller than L_{χ_0}. In other words, it is as if the function $\mathcal{G}(\mathbf{x},t,\mathbf{y},0)$ is a δ function, as it would be for all time in the case where diffusivity was zero. At these early times, therefore, advection dominates the evolution of the scalar field (even though diffusion plays an important role in determining the size of the small but finite region in which $\mathcal{G}$ is significantly different from zero), and, if $\mathcal{G}(\mathbf{x},t,\mathbf{y},0)$ was in regime II for all $\mathbf{x}$, the probability density of scalar concentration, for example, would be that implied by the initial condition.

The effect of diffusion on the scalar field at $\mathbf{x}$ is felt when the domain of influence on $\mathbf{x}$ has evolved to a filament whose length is comparable to L_{χ_0}. Beyond this stage there is increasing cancellation in the integral from different parts of the domain of influence (recall that the integral of the initial concentration field over the domain has been assumed to be zero) and hence decay in time.[9] This occurs within regime II only if L_{χ_0} is significantly less than the length scale of the velocity field L_{flow}. This case is the primary focus of Sukhatme and Pierrehumbert.[12] In this case calculations based on the local stretching theory can give useful quantitative information on the decay of the concentration, at least until the end of regime II is reached. Otherwise, if $L_{\chi_0} \sim L_{\text{flow}}$, the diffusive effects are felt precisely when regime II ends and the approximate description of the function $\mathcal{G}(\cdot)$ by the local stretching theory breaks down.

In regime III the decay of the tracer continues to be governed by the way in which the filamentary domain of influence samples the initial condition and the fact that there is increasingly good cancellation from different parts of the domain. By regime IV the idea of a domain of influence is less helpful and it is better to think of the small remaining inhomogeneities of $\mathcal{G}(\mathbf{x},t,\mathbf{y},s)$ as determining the value of $\chi(\mathbf{x},t)$, given the assumption that the integral of $\chi_0(\mathbf{x})$ over the flow domain is zero. We suggest that the decay of $\chi(\mathbf{x},t)$ in this regime is essentially independent of $\mathbf{x}$. The evidence

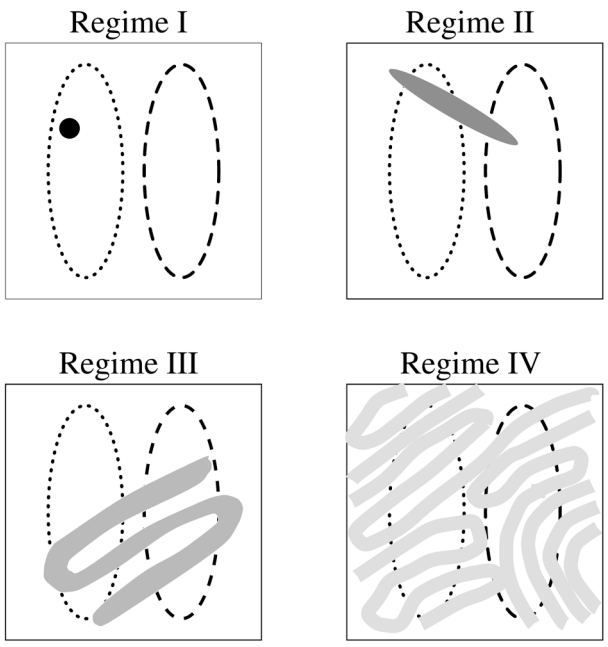

FIG. 1. Schematic diagram showing, in $\mathbf{y}$ space, the different regimes in the evolution of the Green function $\mathcal{G}(\mathbf{x},t,\mathbf{y},s)$ as s decreases from t. Regime I: $[t-s \ll S_{\text{loc}}^{-1}]$ Diffusion dominates and the domain of influence spreads isotropically. Regime II: $\left[S_{\text{loc}}^{-1} \lesssim t-s \ll \frac{1}{2}S_{\text{loc}}^{-1}\ln(S_{\text{loc}}L_{\text{flow}}^2/\kappa)\right]$ The domain of influence is determined by diffusion and the local stretching experienced along the backward trajectory from $\mathbf{x}$. (S_{loc} is the time-averaged stretching rate following the backward trajectory.) Regime III: $\left[\frac{1}{2}S_{\text{loc}}^{-1}\ln(S_{\text{loc}}L_{\text{flow}}^2/\kappa) \lesssim t-s \lesssim S_{\text{glob}}^{-1}\ln(S_{\text{loc}}L_{\text{flow}}^2/\kappa)\right]$ The domain of influence has the form of a filament whose length is larger than the length scale of the flow L_{flow} and which therefore experiences stretching corresponding to several different backward trajectories, represented by an average stretching rate S_{glob}. Regime IV: $[t-s \gtrsim S_{\text{glob}}^{-1}\ln(S_{\text{loc}}L_{\text{flow}}^2/\kappa)]$ The domain of influence covers the whole flow domain, though the function $\mathcal{G}(\mathbf{x},t,\mathbf{y},s)$ is not homogeneous. The elliptical curves are schematic contours of a possible initial condition (applied at $t=s$) with the dotted curve indicating negative values and the dashed curve indicating positive values. The concentration at $\mathbf{x}$ at time t due to this initial condition is the weighted integral of the initial concentration field over the domain of influence.

from numerical solutions (see Sec. IV, Pierrehumbert[9] and Sukhatme and Pierrehumbert[12]) that the integral (2) decays exponentially with time during this regime and that the rate of exponential decrease at large times is independent of initial conditions is entirely consistent with this. While it seems rather clear that the local stretching theories cannot capture all aspects of the behavior in regimes III and IV, it cannot be immediately assumed that all of the predictions of these theories are incorrect. This point will be discussed further later in the paper.

III. LAGRANGIAN STRETCHING THEORIES

During regimes I and II above the behavior of $\mathcal{G}(\mathbf{x},t,\mathbf{y},s)$ may be captured by assuming that that the flow is a linear function of $\mathbf{x}$. Writing $\mathbf{G}(\mathbf{x},t,\mathbf{y},s)=\tilde{\mathcal{G}}(\mathbf{x},t,\mathbf{r},s)$, where $\mathbf{r}=\mathbf{y}-\mathbf{X}(s;\mathbf{x},t)$ and $\mathbf{X}(s;\mathbf{x},t)$ is the position of a diffusionless fluid particle at time s that is at $\mathbf{x}$ at time t, it follows that (3) reduces

$$\tilde{\mathcal{G}}_s+[\sigma(s;\mathbf{x},t)\cdot\mathbf{r}]\nabla_{\mathbf{r}}\tilde{\mathcal{G}}+\kappa\nabla_{\mathbf{r}}^2\tilde{\mathcal{G}}=0, \tag{4}$$

where $\tilde{\mathcal{G}}\to\delta(\mathbf{r})$ as $s\to t^-$ and $\sigma(s;\mathbf{x},t)=\nabla_y\mathbf{u}(\mathbf{y},s)|_{y=\mathbf{X}(s;\mathbf{x},t)}$. [In other words, as s decreases from t, $\sigma(s;\mathbf{x},t)$ is the velocity gradient tensor evaluated along the backwards particle trajectory starting from $\mathbf{x}$.]

Note that to each point $\mathbf{x}$ there corresponds a different backward trajectory $\mathbf{X}(s;\mathbf{x},t)$ and hence a different stretching history defined by the variation of $\sigma(s;\mathbf{x},t)$. The basis of the Lagrangian stretching theories is that the statistical properties of $\chi(\mathbf{x},t)$ (with different values of $\mathbf{x}$ taken as different realizations) may be predicted by considering that, for different $\mathbf{x}$, $\sigma(s;\mathbf{x},t)$ is a different realization of a random function and hence that statistical properties over $\mathbf{x}$ are equivalent to statistical properties over all realizations of this random function.

To make straightforward relation with previous work, we here consider the forward-in-time equation corresponding to (4). [But exactly the same conclusions follow from solving (4) itself.] This may be solved in terms of a time-dependent Gaussian function of space, which is the approach used by Balkovsky and Fouxon.[3] An alternative, but entirely equivalent approach, used by Antonsen *et al.*,[1] is to consider sinusoidal solutions of the form $\chi(\mathbf{x},t)=\mathrm{Re}[\hat{\chi}(\mathbf{k}_0,t)\exp[i\mathbf{k}(t)\cdot\mathbf{x}]]$, where $d\mathbf{k}/dt=-\mathbf{k}.\sigma$, with $\mathbf{k}(0)=\mathbf{k}_0$ and $d\hat{\chi}(\mathbf{k}_0,t)/dt=-\kappa|\mathbf{k}(t)|^2$. If the flow is stretching then $\mathbf{k}(t)$ may be divided into two parts, one of which is exponentially increasing and the other of which is exponentially decreasing, so that $\mathbf{k}(t)=(\mathbf{k}_0\cdot\mathbf{e}_0^+)\mathbf{e}^+(t)e^{ht}+(\mathbf{k}_0\cdot\mathbf{e}_0^-)\mathbf{e}^-(t)e^{-ht}$ where $[\mathbf{e}_0^+,\mathbf{e}_0^-]$ and $[\mathbf{e}^+(t),\mathbf{e}^-(t)]$ are pairs of orthonormal unit vectors and $h>0$. To be precise $\mathbf{e}_0^-$ is the direction at $t=0$ of a solution $\mathbf{k}(t)$ that shrinks in forward time and $\mathbf{e}^+(t)$ is the direction at t of a solution $\mathbf{k}(t)$ that shrinks in backward time. (Note that h is usually t-dependent.) It follows that, at large times, $\hat{\chi}(\mathbf{k}_0,t)\simeq\hat{\chi}(\mathbf{k}_0,0)\exp[-\kappa(\mathbf{k}_0\cdot\mathbf{e}_0^+)^2\int_0^t dt' e^{2h(t')t'}]\simeq\hat{\chi}(\mathbf{k}_0,0)\exp(-\kappa|\mathbf{k}|^2\tau)$ where $\tau=\int_0^t dt' e^{2h(t')t'-2h(t)t}$.

The integral defining τ is dominated by times close to t and Antonsen *et al.*[1] argue that in the large-t limit it is therefore independent of h, which depends on the entire stretching history.

The approach now is to regard h as a random variable whose probability distribution function at large times may be approximated by the "large-deviation" form $P(h,t)\sim\exp[-tG(h)]$, where $G(\cdot)$ is the Cramer "rate function" and τ as an independent random variable whose probability distribution is stationary and represented by the probability density function $M(\tau)$.

Antonsen *et al.*[1] estimate the scalar variance $C_2(t)$ resulting from a sinusoidal initial condition with wavenumber $\mathbf{k}_0$ as

$$C_2(t)=\int_0^\infty dh\int_0^{2\pi}d\theta\int_0^\infty d\tau\frac{1}{2\pi}P(h,t)M(\tau)\times\exp(-2\kappa\cos^2\theta\mathbf{k}_0^2e^{2ht}\tau). \tag{5}$$

Note that the angle between $\mathbf{k}_0$ and $\mathbf{e}_0^+$ has been written as θ and has been assumed to be uniformly distributed in $[0,2\pi)$. Note also that h has been constrained to be positive. Antonsen *et al.*[1] argue that for large times the above integral is dominated by values of θ for which $\cos^2\theta$ is close to zero. It follows that

$$C_2(t)\sim\int_0^\infty dh\exp[-ht-G(h)t]\times\int d\tau\frac{1}{2}\left(\frac{2}{\kappa\pi\mathbf{k}_0^2\tau}\right)^{1/2}M(\tau). \tag{6}$$

(The calculation of Antonsen *et al.*[1] differs in detail here, but the differences have no consequence for what follows.)

The τ integral is constant in time. Noting that the h-integral is for large times dominated by the contribution from the minimum of $h+G(h)$, it therefore follows that $C_2(t)\sim\exp(-\gamma_2 t)$, where $\gamma_2=h_2+G(h_2)$, with h_2 defined by $1+G'(h_2)=0$, assuming that $h_2\geqslant 0$. If h_2 by this definition is less than zero, then the integral is dominated by the contribution from near $h=0$ and $\gamma_2=G(0)$. (This latter possibility is neglected by Antonsen *et al.*[1])

Exactly the same expression for the decay rate of the variance is deduced by Balkovsky and Fouxon,[3] who assume that the initial condition is a Gaussian random function of space, rather than being sinusoidal, and characterize the decay by taking statistical averages over all realizations of this random function. Balkovsky and Fouxon[3] also predict the decay rate of higher moments of the scalar field, for this particular type of initial condition. They show from the relevant generalization of (6) that the decay rate γ_α of the αth moment is given by $\gamma_\alpha=\frac{1}{2}\alpha h_\alpha+G(h_\alpha)$, where $\frac{1}{2}\alpha+G'(h_\alpha)=0$, unless $h_\alpha<0$ in which case $\gamma_\alpha=G(0)$. It follows that γ_α is a nonlinear function of α with γ_α/α decreasing as α increases, and such that γ_α is independent of α for $\alpha\geqslant\alpha_c=-2G'(0)$. The physical reason for this is that, for $\alpha\geqslant\alpha_c$ the decay is controlled by the realizations for which the stretching is zero. The proportion of such realizations decreases exponentially with time at rate $G(0)$.

As noted in Sec. II, the approximations leading to (4) are valid only in regimes I and II and are not justifiable once

regime III is reached. The time to reach regime III is different for different realizations of $\sigma(s;\mathbf{x},t)$. Nonetheless, as shown in the Appendix, even for those (rare) realizations for which there is no stretching at some large time t, diffusive effects alone will have enlarged the domain of influence to an area of at least $\sim\kappa t$. Nothing that the proportion of such realizations decreases as $\exp[-G(0)t]$, it follows that the assumption that solutions of (4) may be treated independently for each $\mathbf{x}$ fails when $t \gtrsim T_{\max}$, where $\kappa T_{\max} \sim L_{\text{flow}}^2 \times \exp(-G(0)T_{\max})$, i.e., when the area of the domain of influence for a single point is larger than the area of the flow corresponding to realizations with zero stretching. $T_{\max}$ is estimated by the expression $T_{\max} \sim G(0)^{-1} \ln[L_{\text{flow}}^2 G(0)/\kappa]$.

IV. NUMERICAL RESULTS ON STRANGE EIGENMODES

In order to support the arguments in Sec. II about the possible shortcomings of the Lagrangian stretching theories at large times and to provide numerical results as a basis for comparison in Sec. VI we now consider explicit numerical simulations of the advection-diffusion equation.

We follow previous authors, including Antonsen *et al.*[1] and Pierrehumbert,[9] in considering a sequence of alternating sinusoidal shear flows (with spatial period 1 in x and y), first in the x direction and then in the y direction. In other words in the interval $n \leqslant t < (n+1)$ the flow is given by

$$\mathbf{u}(\mathbf{x}, n+\tau) = U[f(\tau)\sin[2\pi(y+\phi_n)]\mathbf{e}_x + [1-f(\tau)]\sin[2\pi(x+\psi_n)]\mathbf{e}_y], \tag{7}$$

where $\mathbf{e}_x$ and $\mathbf{e}_y$ are unit vectors in x and y directions, respectively, and $f(\tau)$ is defined by $f(\tau)=1$ $(0<\tau<1/2)$ and $f(\tau)=0$ $(1/2<\tau<1)$. U is a constant specifying the magnitude of the velocity field. The phases ϕ_n and ψ_n are chosen randomly from one value of n to the next. This ensures that there are no transport barriers and that the flow is globally chaotic. For the present we impose the condition that the scalar field has the same spatial periodicity as the velocity field, i.e., that $\chi(x,y,t)=\chi(x+1,y,t)=\chi(x,y+1,t)$.

Following Pierrehumbert[9] we use a "lattice-advection" method to solve the advection-diffusion problem. The advection by the sinusoidal shear over one half interval of length $1/2$ is represented as a mapping on a discrete lattice and used to update the scalar field. This is followed by another mapping on a lattice, representing the effect of a shear in an orthogonal direction to the first, followed by a diffusive step. We chose to implement the diffusive step using a Fourier transform method, rather than as a smoothing operation on the grid, since that allowed a greater range of values of diffusivity to be used. Most results reported below are for calculations on a grid of 1600×1600 points, though sensitivity of increasing the number of grid points was checked and in some cases (e.g., for large values of U) the number was increased, to a maximum of 5000×5000.

This approach to solving the advection-diffusion equation is somewhat crude, since the advection and diffusion steps are both separated and represent effects acting over a finite time interval, but tests conducted with larger numbers of advection and diffusion steps within each time period indicated little quantitative sensitivity to the number of steps. For example, the variance decay rate varied by about 2% as the number of advection and diffusion steps in each time period increased from the minimum described above.

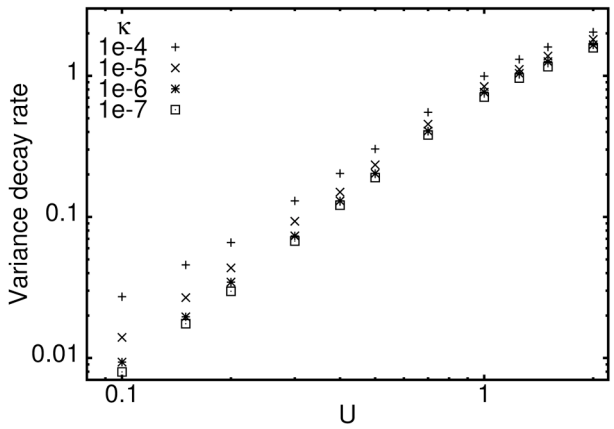

FIG. 2. Variance decay rate as a function of U for four different values of κ.

The decay of the scalar variance in flows such as (7) has been discussed by previous authors and our results confirm their conclusions that the variance decays, on average, exponentially for large times and that the decay rate is independent of the initial condition. Pierrehumbert[10] interpreted this behavior as the emergence of a slowest decaying "strange eigenmode" of the advection-diffusion problem.

It appears from our results that the decay rate γ_2 of the variance appears to tend to a nonzero limit as the diffusivity κ tends to zero, though from the numerical results it is difficult to be precise about the form of the κ dependence. The finite nonzero decay rate as $\kappa\to0$ would not be expected in a flow with barriers to advective transport, i.e., many (and possibly all) time-periodic flows. Pikovsky and Popovych[13] describe explicit calculations suggesting that the decay rate tends to zero as $\kappa\to0$ in such flows.

For reference, it is useful to record the dependence of variance decay rate on U and this is shown in Fig. 2. The asymptotic forms of γ_2 are, for small U, $\gamma_2 \sim 0.75U^2$ and, for large U, $\gamma_2 \sim 1.47\ln U + 0.65$. The coefficients here have been derived from numerical fit, but the forms of the expressions may be justified analytically.

The issue to be considered now is the extent to which this exponential decay is predicted by the Lagrangian stretching theories. Recall first that certain of these theories predict nonlinear dependence on α of the decay rate of the αth moment. In Fig. 3 we show, for various even N, the typical time evolution of the ratio of the Nth moment of the scalar field C_N to the $N/2$th power of the second moment $(C_2)^{N/2}$. According to these theories[2–4] such quantities should increase exponentially with time. However, this is not what is observed. It may be seen from the figure that there are indications of exponential increase up to $t=50$ or so, but beyond that there is no further systematic increase. The fluctuations at later times are associated with the aperiodicity of the flow. (The details of the fluctuations vary from one flow realization to another.)

The behavior of the ratios is consistent with the obser-

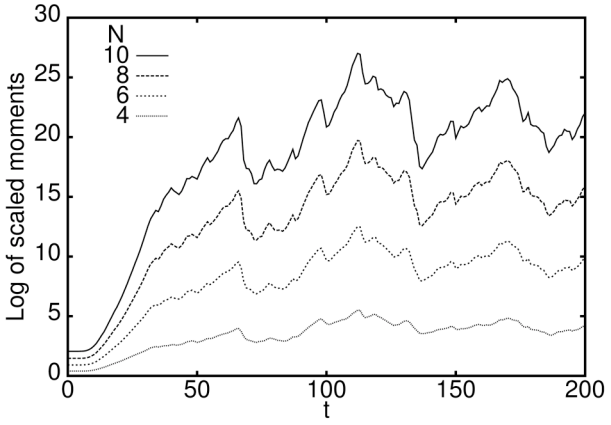

FIG. 3. Plots of the quantities $C_N/C_2^{N/2}$ as a function of time. For these results the initial scalar field is given by $\chi_0=\cos 2\pi x$, with $U=0.5$ and $\kappa=10^{-7}$.

vation by Pierrehumbert[9] that the probability density functions for the scalar field (scaled by the variance) tend to an invariant form. Further detailed evidence on this point is presented by Sukhatme and Pierrehumbert.[12]

An additional aspect of the prediction of decay rate from the Lagrangian stretching theories[1–4] is that there is no reference to boundary conditions on the scalar field. However, if we consider the decay of the scalar in the flow (7), but increase the assumed spatial period P of the scalar field relative to that of the velocity, i.e., apply the condition $\chi(x,y,t)=\chi(x+P,y,t)=\chi(x,y+P,t)$, then the decay rate is found to depend on P, as shown in Fig. 4.

Note that the values of the decay rate when P is large agree with the estimate of $\frac{1}{2}(\pi U/P)^2$ obtained from "homogenization" theories (e.g., Sec. II of the review by Majda and Kramer[14]). This estimate may also be obtained by considering the rate at which variance is transfered out of the gravest spatial mode in the system.

Note that the distribution of stretching factors is independent of P and the Lagrangian stretching theories would therefore predict the decay rate of the variance to also be

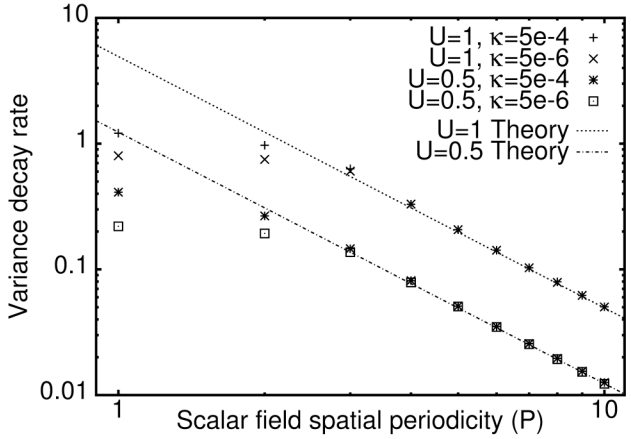

FIG. 4. Variance decay rate as a function of spatial periodicity P for different values of U and κ. The straight lines indicate the decay rate predicted by considering the transfer of variance out of the gravest mode.

independent of P. This clearly indicates that the theoretical prediction of the decay cannot always be correct. (Of course the theories are based on the premise that the important structure in the scalar field is on much smaller scales than those of the velocity field and large values of P would therefore perhaps not be expected to be in the scope of the theories. But nonetheless there is significant dependence of the decay rate on P when P is not large.)

V. CRAMER RATE FUNCTION FOR DISTRIBUTION OF STRETCHING FACTORS

An important aspect of the Lagrangian stretching theories is that the decay rate is predicted in terms of the Cramer rate function $G(\cdot)$ that governs the distribution of stretching factors. Estimation of $G(\cdot)$ by direct simulation of the random process is delicate, since, away from the minimum of $G(\cdot)$, its form is necessarily associated with values that are realized extremely infrequently.

Inspection of Fig. 9 of Antonsen *et al.*[1] suggests that the data used to estimate $G(\cdot)$ is widely scattered on the crucial part of the function. The claimed agreement between the predicted and measured decay rate is crucially dependent on the fitting of a suitable polynomial function to these widely scattered points. Furthermore, the Cramer function plays an important role in the theory developed in Sec. VI. We therefore investigate accurate evaluation of the Cramer function in more detail.

The large-deviation result for the probability density function $P(h,t)$ for h is that

$$P(h,t) \simeq \left(\frac{tG''(h)}{2\pi}\right)^{1/2} \exp[-tG(h)]. \tag{8}$$

Rearranging gives an estimate for $G(h)$ as

$$G(h) \simeq -\frac{1}{t}\ln\left(\frac{P(h,t)}{t^{1/2}}\right) \tag{9}$$

where terms that are $O(t^{-1})$ or smaller have been neglected.

The probability density function $P(h,t)$ was estimated by following infinitesimal material ellipses in the flow defined by (7). The most straightforward simulation of the process described by the ensemble theories would be to follow a large set of such ellipses, each started at a different location in a single flow (i.e., defined by a single sequence $\{\phi_i,\psi_i,i=1,2,\ldots\}$). But it was found that the convergence of the $G(h)$ estimates generated in this manner was very slow. We have noted earlier that we are regarding the decay rate of the variance (and all other moments) as characterizing almost all realizations of the flow and it follows that $P(h,t)$ should be regarded as applying to the entire set of realisations. Therefore the $P(h,t)$ were instead generated by following line elements in different flows (i.e., defined by different sequences $\{\phi_i,\psi_i,i=1,2,\ldots\}$). This gave a more rapidly convergent estimate for $G(h)$ for smaller times. Figure 5 shows the approximations to $G(h)$ generated by Eq. (9) at different times. Convergence of the estimates as time increases is good near the minimum of $G(h)$, but not surprisingly, the number of realizations contributing to the estimate of $G(h)$ away from the minimum, in particular where $G(h)+h$ is a minimum,

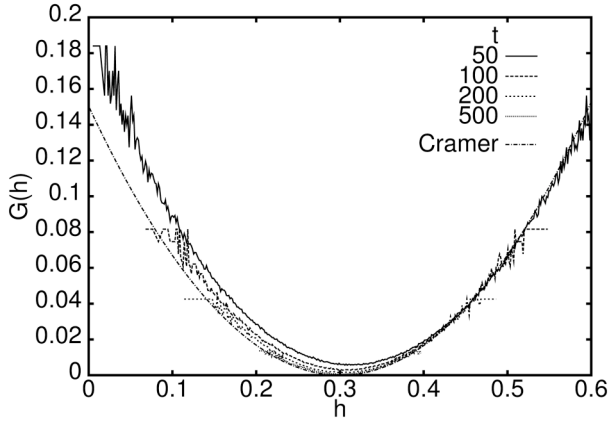

FIG. 5. Comparison of the rate function $G(h)$ for $U=0.5$ generated from the Cramer formula (10) using the estimated probability density function of the stretching factors over ten periods with numerical results based on the asymptotic form for $P(h,t)$ for several different values of t.

significantly decreases as time increases. However estimates at moderate times suggest that the difference between the finite-time estimate for the minimum value of $G(h)+h$ and the infinite-time estimate varies as a negative power of t. This can be used as the basis of improved estimates of γ and, for $U=0.5$, for example, predicted $\gamma_2=0.14$, whereas a simple estimate from the form of $P(h,t)$ for $t=80$ predicted $\gamma_2=0.174$.

A more direct approach to calculating $G(\cdot)$ is based on the probability density function for the underlying random variable (which is the logarithm Λ, say, of the stretching factor over time interval 1). Then $G(\cdot)$ is given by

$$G(h)=\sup_z\{zh-\ln\langle e^{z\Lambda}\rangle\} \tag{10}$$

(the Cramer formula).

One complication here is that the stretching factor over one time interval is not independent of the stretching history in previous time intervals. However a sequence of approximations to the probability density function of Λ may be generated by replacing the $\ln\langle e^{z\Lambda}\rangle$ in (10) by $N^{-1}\ln\langle e^{z\Lambda_N}\rangle$, where Λ_N is the logarithm of the stretching factor over N time intervals, and letting N increase. The moment generating function may be estimated by calculating the expectation over a large number of realizations, for randomly chosen initial conditions and flow history. Close agreement between estimates for $N=5$ and $N=10$ indicate that $N=10$ is sufficiently large for the procedure to have converged. The estimate for $N=10$ is superimposed on Fig. 5 and shows very good agreement with the estimate from (9) for $t=500$, though the latter estimate is useful only close to the minimum of $G(h)$. The $N=10$ estimate for $G(h)$ implies that $\gamma_2=0.15$. It also appears that the relevant value of h [i.e., that for which $G'(h)=-1$] is very close to zero.

We therefore have that our two most reliable estimates of $G(h)$ for $U=0.5$ imply, respectively, $\gamma_2=0.14$ and $\gamma_2=0.15$. It has not been possible to obtain convincing evidence that these are significantly different from the simulated decay rate, with part of the difficulty being the extrapolation to $\kappa=0$. Thus, while the results shown in Fig. 4 show that the variance decay rate is not predicted correctly by the Lagrangian stretching theories for all flows, results from numerical simulation indicate that the decay rate is predicted correctly for some flows, in particular for the case $P=1$ considered by Antonsen *et al.*[1]

VI. PROPERTIES OF THE SCALAR FIELD IN THE STRANGE EIGENMODE PHASE

The results of Sec. IV show that in some cases the decay rate of the variance cannot be captured by the Lagrangian stretching theories and is determined by the action of the flow on the largest scales in the tracer field. This suggests that the corresponding predictions for wavenumber spectrum[1] and for probability density functions for scalar concentration[3,9] need reexamination. In this section we set out alternative theories for these quantities and test against the numerical simulations.

A. Wavenumber spectrum of scalar field

The wavenumber spectrum of the decaying scalar has been predicted by Antonsen *et al.*[1] based on the Lagrangian stretching theories. The evidence from previous sections is that, in some flows at least, this prediction cannot be correct. However the corresponding theory for the steady-state forced problem (where the spatial contrast in the scalar is forced at large scales) is useful (see further comments in Sec. VII), and it turns out that extension is also relevant to the spatially decaying problem of interest here.

As explained in Sec. III, the basis of the Lagrangian stretching theories is that a scalar Fourier component with initial form $\hat{\chi}(\mathbf{k}_0,0)\exp(i\mathbf{k}_0\cdot\mathbf{x})$ has at later time, t, the form $\hat{\chi}(\mathbf{k}_0,0)\exp(-\kappa|\mathbf{k}(t)|^2\tau)\exp(i\mathbf{k}(t)\cdot\mathbf{x})$, where $|\mathbf{k}(t)|=k_0\cos\theta e^{ht}$ and τ and h may, at large times, be regarded as independent random variables with probability density functions $M(\tau)$ and $P(h,t)$ respectively. It follows, as for the expression (5), that the power spectrum at time t of the scalar field that initially consists of this single Fourier component is given by

$$E(k,t)=\int_0^\infty dhP(h,t)\int_0^\infty d\tau M(\tau)\int_0^{2\pi}\frac{d\theta}{2\pi}\exp(-2\kappa k_0^2\tau\times\cos^2\theta e^{2ht})\delta(k-k_0|\cos\theta|e^{ht}). \tag{11}$$

The approach of Antonsen *et al.*[1] is to evaluate this at large times by integrating over θ and h, using the large-deviation asymptotic expression for $P(h,t)$ as described in Sec. III to give

$$E(k,t)\sim\exp(-\gamma_2^*t)\int_0^\infty\exp(-2\kappa k^2\tau)M(\tau)d\tau, \tag{12}$$

where γ_2^* is the decay rate of the variance predicted by the Lagrangian stretching theory. [Note that the formula for $E(k,t)$ given by Antonsen *et al.*[1] is missing the factor of 2 in the $\exp(-2\kappa k^2\tau)$ term.] Given that the actual decay rate γ_2 is not always equal to the predicted decay rate γ_2^*, the expression (12) cannot always be correct. The arguments given in Sec. II suggest that one problem is that the approximations

made in the Lagrangian stretching theories apply only for finite time.

Consider now the forced case, where scalar variance at wavenumber $\mathbf{k}_0$ is continually added to the system. As argued by Antonsen *et al.*,[1] the corresponding power spectrum may be found by integrating Eq. (11) with respect to time as follows:

$$\begin{aligned} E(k,t) &= \int_{-\infty}^{t} ds \int_0^{\infty} dh P(h,t-s) \int_0^{\infty} d\tau M(\tau) \\ &\quad \times \int_0^{2\pi} \frac{d\theta}{2\pi} \exp(-2\kappa k_0^2 \tau \cos^2\theta \exp 2h(t-s)) \\ &\quad \times \delta(k - k_0|\cos\theta| e^{h(t-s)}) \\ &= \int_0^{\infty} ds \int_0^{\infty} dh P(h,s) \int_0^{\infty} d\tau M(\tau) \int_0^{2\pi} \frac{d\theta}{2\pi} \\ &\quad \times \exp(-2\kappa k_0^2 \tau \cos^2\theta \exp 2hs) \\ &\quad \times \delta(k - k_0|\cos\theta| e^{hs}). \end{aligned} \tag{13}$$

The second expression is independent of time, implying that the forced power spectrum evolves to a steady state, in which the variance added at the low wavenumber k_0 is balanced by the variance dissipated at high wavenumbers. For given k, the integral is dominated by the contribution from finite s, since the transfer of scalar variance from the forcing wavenumbers k_0 to any finite higher wavenumber k takes place over a finite time scale. Thus it is the finite-time behavior of (11) that determines the form of (13), and (13) is therefore potentially useful whether or not the validity of (11) breaks down at large times. (Again, see further discussion in Sec. VII.)

Integrating the δ function over s gives

$$\begin{aligned} E(k,t) &= \frac{1}{k} \int_0^{2\pi} \frac{d\theta}{2\pi} \int_0^{\infty} dh \frac{1}{h} P\left(h, \frac{\ln(k/k_0|\cos\theta|)}{h}\right) \\ &\quad \times \int_0^{\infty} d\tau M(\tau) \exp(-2\kappa k^2 \tau). \end{aligned}$$

For sufficiently large k, the probability density function for h may, in this case, be approximated by $P \sim \delta(h - h_{\text{avg}})$, where h_{avg} is the mean stretching rate, so that

$$\int_0^{\infty} dh \frac{1}{h} P\left(h, \frac{\ln(k/k_0|\cos\theta|)}{h}\right) \simeq \frac{1}{h_{\text{avg}}},$$

hence

$$E(k,t) \sim \frac{1}{k h_{\text{avg}}} \int_0^{\infty} d\tau M(\tau) \exp(-2\kappa k^2 \tau). \tag{14}$$

This is the well-known k^{-1} Batchelor spectrum, modified by diffusion. (See also Yuan *et al.*,[15] Haynes and Vanneste.[16]) The accuracy of this prediction has been tested by generating $M(\tau)$ numerically and using it to calculate the predicted $E(k,t)$. The predicted $E(k,t)$ is close to the $E(k,t)$ measured in scalar field simulations for a variety of different values of κ and U. In the simulation the forcing is implemented by adding to the scalar field an increment proportional to $\cos 2\pi x$ at each time step. For U small, the power spectra seen in the scalar field simulations fluctuate over time. However, the predicted power spectrum appears to be within the range of these fluctuations. The good agreement between simulation and theory in the forced case has already been demonstrated by Antonsen *et al.*[1]

The possibility has been raised by the results in Sec. IV that in some cases the decay rate is determined at large scales. This motivates a heuristic extension to the freely decaying case of the above theory for the spectrum in the forced case, by regarding the variance at low wavenumbers as providing a forcing whose variance decays exponentially in time as $\exp(-\gamma_2 t)$. For the freely decaying problem, we therefore expect the spectrum to be predicted a similar expression to (13), but including a term $\exp(-\gamma_2 s)$ in the s-integral to account for the time decay:

$$\begin{aligned} E(k,t) &= \int_{-\infty}^{t} ds \exp(-\gamma_2 s) \int_0^{\infty} dh P(h,t-s) \\ &\quad \times \int_0^{\infty} d\tau M(\tau) \int_0^{2\pi} \frac{d\theta}{2\pi} \exp\big(-2\kappa k_0^2 \tau \\ &\quad \times \cos^2\theta \exp 2h(t-s)\big) \\ &\quad \times \delta(k - k_0|\cos\theta| e^{h(t-s)}). \end{aligned} \tag{15}$$

As in the derivation of (13) for the forced case, the potential breakdown of approximations leading to (11) at large time is circumvented by the fact the integral (15) is dominated by finite times.

Integrating over s as before gives

$$\begin{aligned} E(k,t) &= \frac{e^{-\gamma_2 t}}{k} \int_0^{2\pi} \frac{d\theta}{2\pi} \int_0^{\infty} dh \frac{1}{h} \left(\frac{k}{k_0|\cos\theta|}\right)^{\gamma_2/h} \\ &\quad \times P\left(h, \frac{\ln(k, k_0|\cos\theta|)}{h}\right) \\ &\quad \times \int_0^{\infty} d\tau M(\tau) \exp(-2\kappa k^2 \tau). \end{aligned}$$

This integral may now be estimated by writing the second two terms in the h integral as $\exp[-\ln(k/k_0|\cos\theta|)(G(h) - \gamma_2)/h]$ and noting that the dominant contribution comes from $h = h_*$, where $G(h_*) - h_* G'(h_*) - \gamma_2 = 0$ (following Reyl, Antonsen, and Ott[17] who considered the analogous problem for magnetic field). Then, provided $\gamma_2 < h_* + G(h_*)$ (so that the singularities of $|\cos\theta|^{(G(h_*)-\gamma_2)/h_*}$ are integrable in θ) this gives

$$E(k,t) \sim e^{-\gamma_2 t} k^{-1-G'(h_*)} \int_0^{\infty} d\tau M(\tau) \exp(-2\kappa k^2 \tau), \tag{16}$$

i.e., a similar form as for the forced case, but with a time-decay factor and with a different exponent for the power of k outside the integral. Note that the spectrum in the decaying case is shallower than that in the forced case, and if κ is sufficiently small that there is a range of $k \gg k_0$ such that the exponential decay factor can be ignored then the spectrum is a power law with exponent $-1 - G'(h_*)$, analogous to that

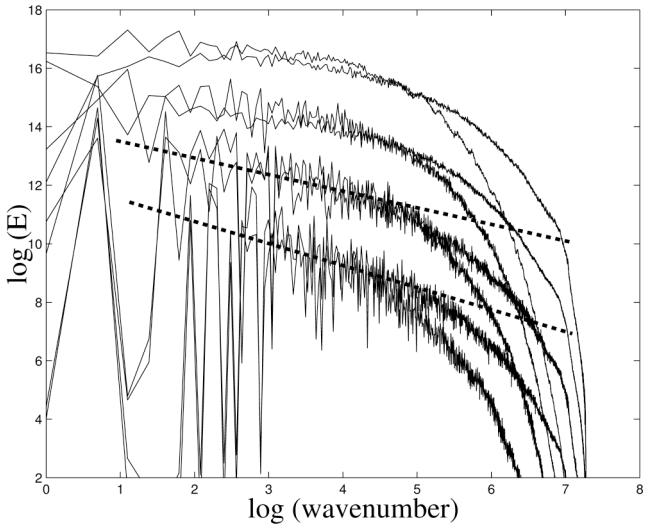

FIG. 6. Wavenumber spectra at large times, suitably normalized, for 2048 $\times$2048 numerical simulations with $U=0.5$ and $P=1,3,5,7$. The graphs are offset with $P=1$ the uppermost and $P=7$ the lowermost. For each P two cases are shown, one with $\kappa=10^{-7}$ and the other with $\kappa=3\times10^{-8}$, to give a sense of the effect of diffusivity. The significant differences between decay rates for $P=5$ and $P=7$ on the one hand and $P=1$ on the other, suggests that the formula (16) applies to the former two cases. The numerically calculated decay rates and the function $G(\cdot)$ shown in Fig. 5 imply that the prefactor of the expression (16) should be $k^{-0.6}$ for $P=5$ and $k^{-0.8}$ for $P=7$. Corresponding dashed lines are superimposed in the figure.

found by Fereday *et al.*[8] in the one-dimensional baker map problem.

In a case where γ_2 is correctly predicted by the Lagrangian stretching theories, then $\gamma_2=h_*+G(h_*)$ and $G'(h_*)=-1$ and the singularities are not integrable in θ, although a naive interpretation of the previous result would be that the exponent of k is in that case zero, matching the Antonsen *et al.*[1] result. [The requirement for integrability in θ may alternatively be interpreted as implying that the actual decay rate γ_2 can be no larger than that predicted by the Lagrangian stretching theories (E. Ott, personal communication; Tsang *et al.*, paper in preparation)]. If γ_2 is very small, as it would be, for example, in the case studied in Sec. IV if P was very large, then h_* is very close to the minimum of $G(\cdot)$ and $G'(h_*)$ is also very small. Thus if P increases from 1 (when the Lagrangian stretching theory prediction is apparently correct, or at least very accurate) to a large value, the power of k appearing as a prefactor to (16) is predicted by the above calculation to decreases from zero towards -1. Spectra generated by numerical simulations for $P=1$, 3, 5, 7 shown in Fig. 6 appear generally consistent with this prediction, if we consider that the cases $P=5$ and $P=7$ (for which the decay rate is significantly different to that for $P=1$ and $P=3$) are not described by the Lagrangian stretching theory. However the effects of diffusivity limit the range of wavenumbers for which power-law behavior is relevant. The full predicted form (16) may be calculated and is in good agreement with results of explicit numerical simulations for many values of U and κ. Note that Pierrehumbert[9] suggested that the spectrum of the strange eigenmode appeared to have exponential form. Numerical results indicate that for certain parameter values part of the spectrum may be approximated as an exponential function, but no more than that.

The approach to calculating the spectrum outlined above is heuristic, but gives results in good agreement with numerical integration. A more rigorous approach is possible in which the change in the spectrum or second-order structure function over some finite time is considered and combined with the assumption of an exponentially decaying mode.

B. Probability density function for scalar concentration

The probability density function for the scalar concentration may be straightforwardly evaluated from results of numerical simulations. At large times the probability density functions have long tails and can be strongly asymmetric, i.e., with a longer tail for positive values of scalar concentrations and a short tail for negative values, or vice versa. The tails are subject to fluctuations, so that the probability density function can change over time from having a long positive tail to having a long negative tail, and vice versa. The probability density function for the modulus of concentration becomes approximately self similar at large times, in the sense that appropriately normalizing the argument of the probability density function by its standard deviation (to take account of the fact that the scalar field is decaying) produces a function that is approximately time independent. Explicit results are shown by Pierrehumbert[9] and Sukhatme and Pierrehumbert.[12] The self-similar form of the probability density function is consistent with the linear dependence on α of the decay rate of the αth moment.

From (2) we need to consider the probability density function for the quantity

$$\chi(\mathbf{x},t)=\int d\mathbf{y}\chi_0(\mathbf{y})\mathcal{G}(\mathbf{x},t,\mathbf{y},0). \tag{17}$$

We have noted in Sec. II that the evolution of this quantity falls into four stages. For regimes I and II it remains roughly constant, then in regime III it decays as the domain of influence forms an elongated filament that samples many values of the initial concentration $\chi_0(\mathbf{x},t)$. Finally in regime IV, on the evidence presented in Sec. IV, it appears that the integral will decay exponentially at a rate $\frac{1}{2}\gamma_2$ (γ_2 is the decay rate of the variance) that is independent of $\mathbf{x}$. We expect that the time spent in regimes I and II is strongly dependent on $\mathbf{x}$ (it will be long for backward trajectories that experience little stretching) and that the time spent in regime III is more weakly dependent on $\mathbf{x}$ (since the filamental domain of influence experiences stretching histories for many independent backward trajectories in this regime).

Pierrehumbert[9] and Sukhatme and Pierrehumbert[12] have characterized the tail of the probability density function as "stretched exponential" but we argue below that the tail is in fact algebraic. The arguments given by Pierrehumbert[9] for the probability density function are based on the Lagrangian stretching histories and therefore apply only to regimes I and

II. Indeed Sukhatme and Pierrehumbert[12] apply these arguments only to their early-time and intermediate-time regimes.

In order to capture the decay beyond regimes I and II we make the following hypothesis. A random variable representing the concentration $\chi(\mathbf{x},t)$ at large times may be constructed in the form $Z\exp\left[-\frac{1}{2}\gamma_2(t-T_*)\right]$ where Z is a random variable that represents the variation of $\chi_0(\mathbf{x})$ and also variation associated with the passage through regime III. T_* on the other hand, is a random variable representing the time spent in regimes I and II. If the tails of the distribution of Z decay sufficiently rapidly then the tails of the distribution of concentration will be dominated by the tails of the distribution of $\exp\left(\frac{1}{2}\gamma_2 T_*\right)$.

The variable T_* is precisely the variable that appears in the forced problem considered by Balkovsky and Fouxon[3] [defined by their Eq. (4.4)], where it is the time over which the forcing must be integrated to give the value of scalar concentration. Balkovsky and Fouxon[3] have argued that its probability density function at large values may be approximated by $C\exp[-G(0)T_*]$, where C is a constant and $G(\cdot)$ is the Cramer function for the stretching rates, introduced in Sec. III. If follows that the probability density function for $\zeta=\exp\left(\frac{1}{2}\gamma_2 T_*\right)$ may be approximated by $\zeta^{-1-2G(0)/\gamma_2}$, implying that the probability density function for concentration has tails that are algebraically decaying.

An alternative argument for the form of the tail of the probability density function, which exploits the self-similarity, is as follows. Consider the evolution of the pdf between the times t_0 and $t_0+\mathcal{T}$, where t_0 is taken to be sufficiently large that the scalar field has evolved into the long time eigenmode regime. Let the probability density function for scalar concentration at time t be denoted by $\mathcal{P}(c,t)$. Assuming self-similarity, as discussed above, implies that

$$\mathcal{P}(c,t_0+\mathcal{T}) = e^{\gamma_2\mathcal{T}/2}\mathcal{P}(ce^{\gamma_2\mathcal{T}/2},t_0). \tag{18}$$

Now consider the region of influence of the Green's function $\mathcal{G}(\mathbf{x},t_0+\mathcal{T},\mathbf{y},t_0)$ that relates the scalar field at time $t_0+\mathcal{T}$ to that at t_0. By the arguments given in Sec. III, the largest values of scalar concentration at time $t_0+\mathcal{T}$ will be associated with those points $\mathbf{x}$ for which the region of influence of the Green's function is in regime I or II, rather than III or IV. The proportion of such $\mathbf{x}$ is, by the arguments of Balkovsky and Fouxon mentioned above, proportional to $\exp(-G(0)\mathcal{T})$. Assuming that there is no correlation between the regions of influence of such $\mathbf{x}$ and the scalar field at time t_0, it follows that

$$\mathcal{P}(c,t_0+\mathcal{T}) \sim e^{-G(0)\mathcal{T}}\mathcal{P}(c,t_0) \tag{19}$$

for the tails of the scalar pdf. Combining Eq. (18) and (19) implies that $\mathcal{P}(c,t_0)\sim c^{-\beta}$, where $\beta=1+2G(0)/\gamma_2$.

Probability density functions evaluated from the numerical simulations are shown in Fig. 7 and 8 and are clearly consistent with the above prediction of algebraic tails. Furthermore the calculated $G(\cdot)$ curves presented in Sec. V showed that $G(0)/\gamma_2\simeq 1$ for the flows considered here, and hence imply that $\beta\simeq -3$. Again, this appears to be in good agreement with the numerical results.

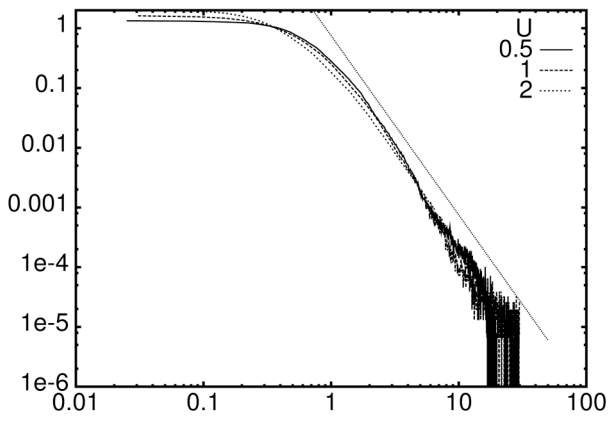

FIG. 7. Probability density function of $|\chi|$ generated by numerical simulation, for different values of U. The straight line indicates a -3 power law.

Finally, consider the effect of diffusivity on the probability density function. From the above it appears that the form of the tails should not depend on the diffusivity. However the argument given at the end of Sec. II suggests that T_* may be no larger than $G(0)^{-1}\ln[L^2G(0)/\kappa]$ and hence that ζ may be no larger than $[L_{\text{flow}}^2G(0)/\kappa]^{\gamma_2/2G(0)}$. The diffusivity therefore determines the position of the cutoff in the tail in the probability density function and increasing the diffusivity moves the cutoff to smaller values. If $G(0)/\gamma_2\simeq 1$, then the value at which the cutoff occurs is proportional to $\kappa^{-1/2}$. The numerical results shown in Fig. 8 are consistent with these theoretical predictions.

VII. DISCUSSION AND CONCLUSIONS

The conclusion of this paper is that, in the initial-value problem, the predictions of Lagrangian stretching theories for the statistics of the scalar field are incorrect in that they do not capture all aspects of the evolution of the scalar field at large times. The reason is that some aspects of the large-time behavior depends on behavior of solutions of the advection-diffusion equation that is not captured by a local

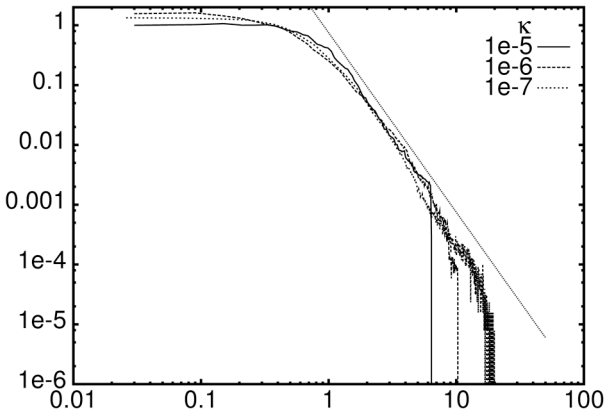

FIG. 8. Probability density function of $|\chi|$ generated by numerical simulation, for different values of κ. Once again the straight line indicates a -3 power law. The variation with diffusivity of the cutoff in the probability density function at large values agrees well with the theoretical prediction.

analysis. These conclusions are supported by the first principles arguments of Secs. II and III, by the demonstration that decay rate of the Nth moment of the scalar ultimately decays at a rate proportional to N (Fig. 3) and by the demonstration that the decay rate depends on the boundary condition applied by the scalar field (Fig. 4). However comparison between predicted decay rates based on a careful calculation of the Cramer function $G(h)$ and decay rates in simulations indicates that the Lagrangian stretching theories do for some classes for flows predict the correct decay rate of the variance. Why the decay rate is predicted correctly for some flows and not for others is under investigation (Tsang *et al.*, Haynes and Vanneste, papers in preparation). The arguments of Secs. II and III have been used to derive updated theories for the wavenumber spectrum of the scalar field and a theory for the probability density of the scalar concentration, which have been shown to be in good agreement with numerical simulation. These derivations exploit some aspects of the Lagrangian stretching theories but, crucially, only in representing the action of the flow over finite times (corresponding to regimes I and II as described in Sec. II).

The discussion so far has focussed on the initial-value problem. The Lagrangian stretching theories have also made predictions about the forced problem, i.e., when the evolution equation for the scalar concentration is

$$\chi_t + \mathbf{u}(\mathbf{x},t)\,.\,\boldsymbol{\nabla}_{\mathbf{x}}\chi - \kappa\boldsymbol{\nabla}_{\mathbf{x}}^2\chi = \phi(\mathbf{x},t) \tag{20}$$

with the forcing $\phi(\mathbf{x},t)$ a given function of space and time. Again it is useful to assume that the integral of $\phi(\mathbf{x},t)$ over the domain is zero.

The solution to (20) may be written as

$$\chi(\mathbf{x},t) = \int_{-\infty}^{t} ds \int d\mathbf{y}\,\phi(\mathbf{y},s)\mathcal{G}(\mathbf{x},t,\mathbf{y},s), \tag{21}$$

where the Green's function is as defined in Sec. II. Note that the solution now involves a time integral (over all previous times) as well as a space integral.

Following the discussion given in Sec. II, we expect the integrand $\int d\mathbf{y}\phi(\mathbf{y},s)\mathcal{G}(\mathbf{x},t,\mathbf{y},s)$ to remain roughly constant as s decreases through regime I and II, until the domain of influence on $\mathbf{x}$ at t is a filament of length comparable to the length comparable to the length scale on which $\phi(\mathbf{x},t)$ varies, after which the integrand will decrease rapidly. If the length scale of the forcing is less than that of the flow, then the value of s at which the integrand begins to decay rapidly will lie within regime II otherwise it will lie precisely at the boundary of regime II and regime III. But once regime III has been entered, the integrand will certainly be decreasing rapidly as s decreases. This suggests that the Lagrangian stretching theories will be able to capture some of the leading order behavior of the scalar field, since the approximate form of $\mathcal{G}(\mathbf{x},t,\mathbf{y},s)$ on which the ensemble theories rely is valid for almost the entire range of s which dominates the integral (21). At first sight, then, we have no reason to disagree with many of the predictions concerning the statistics of the scalar concentration field in the forced problem made by Balkovsky and Fouxon[3] and others. Indeed these predictions seem likely to hold even if the scale of the forcing is the same as the scale of the flow. However the analysis presented in this paper suggests that some modification is needed to take account of the maximum possible value of the time T_* spent in regimes I and II. For example, including this in the analysis of Balkovsky and Fouxon[3] implies that the predicted exponential tails to the probability density function for the scalar concentration have a cut-off at a value of concentration that is proportional to $[\ln(L_{\text{flow}}^2 G(0)/\kappa]$, not proportional to $L_{\text{flow}}^2 G(0)/\kappa$ as suggested previously.[4] Since the value of concentration at which the exponential tails appear has a similar dependence on κ, this might imply that the tails are in practice difficult to observe and in that respect would be consistent with numerical results in Ref. 9. This topic will be analyzed more carefully in future work.

It follows from our conclusions that "verifications" of the Lagrangian stretching theories for the initial value problem by comparison with numerical simulation or experiment need to be interpreted with care. Note, in particular, the paper of Groisman and Steinberg,[18] cited by Falkovich *et al.*,[14] which describes experiments where an elastic fluid (a polymer solution) flows down a contorted pipe and hydrodynamic instabilities driven by the elasticity give rise to efficient mixing. The mixing of a scalar is followed by dyeing part of the flow at one end of the pipe and analyzing the variation of the dye field along the pipe. There is therefore a rough analogy between distance along the pipe in the experiments and time in the initial value problem and Groisman and Steinberg base their comparison between experiments and theoretical predictions on this analogy and present evidence that the decay rate of the moments of the dye concentration along the pipe is a nonlinear function of the index of the moment in agreement with the Lagrangian stretching theories. But the evidence presented above and in Pierrehumbert[9] and Sukhatme and Pierrehumbert[12] is that the decay rate should be a linear function of the moment index. Groisman and Steinberg also present the pdfs of dye concentration and show that they have exponential tails, claiming agreement with the Lagrangian stretching theories. But the Lagrangian stretching theories predict exponential tails only for the forced problem and we have shown above that in the initial value problem the tails are actually algebraic. Other experimental investigations, e.g., Julien, Castiglione, and Tabeling[19] have attempted to identify properties predicted for the forced problem (e.g., k^{-1} spectrum, exponential tails for probability distributions) by selecting a suitable time during an initial value problem. (The forced problem is very difficult to realise in laboratory experiments.) A further important point (perhaps more important than those raised above) noted by Chertkov and Lebedev[20] is that the no-slip condition relevant in laboratory experiments (but not neccessarily in numerical simulations or in geophysical contexts) may significantly effect the decay. Any theory that is to be usefully compared to the experiments must clearly take this into account.

ACKNOWLEDGMENTS

Conversations (many at the 2001 Cargese Summer School on transport and mixing directed by B. Legras) and

correspondence with G. Falkovich, R. Pierrehumbert, A. Schekochihin, J. Sukhatme, T. Tel, J. Vanneste, and M. Vergassola are gratefully acknowledged. Comments by E. Ott on a previous version of the paper were very helpful, particularly in arriving at the formula (16). D.R.F. was supported by a Ph.D. studentship from the UK Natural Environment Research Council while carrying out this work.

APPENDIX: LOWER BOUND ON AREA OF DOMAIN OF INFLUENCE

We consider the solution to (4). First note that the dependence on $\mathbf{x}$ and t is purely parametric. We therefore suppress the $\mathbf{x}$ and t dependence and regard σ solely as a function of s. Then, following solution of the forward time advection-diffusion problem,[3] we note that there is a solution of the form $\tilde{\mathcal{G}}(\mathbf{r},s)=(\det A)^{1/2}\exp(-\mathbf{r}^T A\cdot\mathbf{r})$, where A is a symmetric tensor. It is convenient to define the tensor $B=\int \mathbf{r}\mathbf{r}\tilde{\mathcal{G}}(\mathbf{r},s)d^2\mathbf{r}$ and it follows that $B_{ij}A_{jk}=\delta_{ik}$ and that $B_s=\sigma B+B^T\sigma^T-2\kappa I$, with $B\to 0$ as $s\to t^-$.

Now note that $(\det B)_s=(B_{ij})_s C_{ij}$, where C_{ij} is the cofactor of B_{ij}. Hence

$$(\det B)_s=\sigma_{ik}B_{kj}C_{ij}+\sigma_{jk}B_{ik}C_{ij}-2\kappa C_{jj}$$
$$=\sigma_{ik}\delta_{ik}\det B+\sigma_{jk}\delta_{ik}\det B-2\kappa C_{jj}=-2\kappa C_{jj},$$

where the second equality follows from the identity that $B_{kj}C_{ij}=\delta_{ik}\det B$ (with δ_{ik} the Kronecker delta) and the third equality follows from the incompressibility condition that $\sigma_{ii}=0$.

Now, choosing axes in which B is diagonal and taking λ_1 and λ_2 to be the eigenvalues, it follows that

$$(\lambda_1\lambda_2)_s=-2\kappa(\lambda_1+\lambda_2)\leqslant -4\kappa(\lambda_1\lambda_2)^{1/2},$$

where the second inequality follows from the arithmetic/geometric mean inequality, together with the fact that λ_1 and λ_2 are both positive (since the tensor B is positive definite by definition). The above equation may be written as

$$(\det B)_s\leqslant -4\kappa(\det B)^{1/2}$$

and it therefore follows that $(\det B)^{1/2}\geqslant 2\kappa(t-s)$, using the fact that $\det B=0$ when $s=t$.

Now $(\det B)^{1/2}$ is proportional to the area over which $G(\mathbf{r},s)$ exceeds a certain fraction of its maximum value, i.e., it estimates of the area of the domain of influence. It follows that this area is at given s at least as large as it would have been in the absence of a velocity gradient (in which case it would have increased linearly at rate 2κ as s decreased from t).

It follows that the area of the domain of influence of any point must be at least as large as the area of the flow domain that has experienced zero stretching when $\kappa(t-s)\simeq L_{\text{flow}}^2\exp[-G(0)(t-s)]$.

[1] T. M. Antonsen, Jr., Z. Fan, E. Ott, and E. Garcia-Lopez, "The role of chaotic orbits in the determination of power spectra of passive scalars," Phys. Fluids **8**, 3094 (1996).
[2] D. T. Son, "Turbulent decay of a passive scalar in the Batchelor limit: Exact results from a quantum-mechanical approach," Phys. Rev. E **59**, R3811 (1999).
[3] E. Balkovsky and A. Fouxon, "Universal long-time properties of Lagrangian statistics in the Batchelor regime and their application to the passive scalar problem," Phys. Rev. E **60**, 4164 (1999).
[4] G. Falkovich, K. Gawedzki, and M. Vergassola, "Particles and fields in fluid turbulence," Rev. Mod. Phys. **73**, 913 (2001).
[5] H. Aref, "Stirring by chaotic advection," J. Fluid Mech. **143**, 1 (1984).
[6] J. M. Ottino, *The Kinematics of Mixing: Stretching, Chaos and Transport* (Cambridge University Press, Cambridge 1989).
[7] S. Wiggins, *Chaotic Transport in Dynamical Systems* (Springer, Berlin, 1991).
[8] D. R. Fereday, P. H. Haynes, A. Wonhas, and J. C. Vassilicos, "Scalar variance decay in chaotic advection and Batchelor-regime turbulence," Phys. Rev. E **65**, 035301 (2002).
[9] R. T. Pierrehumbert, "Lattice models of advection-diffusion," Chaos **10**, 61 (2000).
[10] R. T. Pierrehumbert, "On tracer microstructure in the large-eddy dominated regime," Chaos, Solitons Fractals **4**, 1091 (1994).
[11] S. Childress and A. D. Gilbert, *Stretch, Twist, Fold: The Fast Dynamo* (Springer, Berlin, 1995).
[12] J. Sukhatme and R. T. Pierrehumbert, "Decay of passive scalars under the action of single scale smooth velocity fields in bounded two-dimensional domains: From non-self-similar probability distribution functions to self-similar eigenmodes," Phys. Rev. E **66**, 056302 (2002).
[13] A. Pikovsky and O. Popovych, "Persistent patterns in deterministic mixing flows," Europhys. Lett. **61**, 625 (2003).
[14] A. J. Majda and P. R. Kramer, "Simplified models for turbulent diffusion: Theory, numerical modelling and physical phenomena," Phys. Rep. **314**, 237 (1999).
[15] G-C. Yuan, K. Nam, T. M. Antonsen, Jr., E. Ott, and P. N. Guzdar, "Power spectrum of passive scalars in two dimensional chaotic flows," Chaos **10**, 39 (2000).
[16] P. H. Haynes and J. Vanneste, "Stratospheric tracer spectra," J. Atmos. Sci. **61**, 161 (2004).
[17] C. Reyl, T. M. Antonsen, Jr., and E. Ott, "Scaling properties of magnetic dynamo wavenumber power spectra generated by Lagrangian chaotic flow," Phys. Plasmas **5**, 151 (1998).
[18] A. Groisman and V. Steinberg, "Efficient mixing at low Reynolds numbers using polymer additives," Nature (London) **410**, 905 (2001).
[19] M.-C. Julien, P. Castiglione, and P. Tabeling, "Experimental observation of Batchelor dispersion of passive tracers," Phys. Rev. Lett. **85**, 3636 (2000).
[20] M. Chertkov and V. Lebedev, "Decay of scalar turbulence revisited," Phys. Rev. Lett. **90**, 034501 (2003).